

COMPARISON AND OPTIMIZATION OF DISPERSION, AND LOSSES OF PLANAR WAVEGUIDES ON BENZOCYCLOBUTENE (BCB) AT THZ FREQUENCIES: COPLANAR WAVEGUIDE (CPW), MICROSTRIP, STRIPLINE AND SLOTLINE

Lei Cao, Anne-Sophie Grimault-Jacquin^{*}, and Frédéric Aniel

IEF CNRS UMR 8622, Université Paris Sud, Bât. 220 91405 Orsay Cedex, France

Abstract—This paper proposes an investigation in the terahertz (THz) frequency range of the dispersion and an individual quantitative treatment of the losses of the most classical microwave waveguides (coplanar, slotline, microstrip and stripline) numerically led in three dimensions (3D). An original strategy has been used to quantify radiation losses associated with leaky modes. A very low THz permittivity polymer (benzocyclobutene (BCB)) was used as a very convenient substrate to be easily grafted as a THz environment of integrated passive or/and active devices. Direct comparisons of the losses and the dispersion have been performed following two criteria: a constant characteristic impedance Z_c fixed at $100\ \Omega$ and a constant effective width W_{eff} fixed at $30\ \mu\text{m}$. The best waveguides are microstrip ($\alpha_T = 2.52\ \text{dB/mm}$ for $Z_c = 100\ \Omega$ and for $W/H = 35/50\ \mu\text{m}$ (with W the strip width and H the substrate height) and $\alpha_T = 2.29\ \text{dB/mm}$ for $W_{eff} = 30\ \mu\text{m}$ at 1 THz with $H = 30\ \mu\text{m}$) and stripline (with quasi-null radiation losses and the best quality factor $Q_T = 63$ for $Z_c = 100\ \Omega$). The large dispersion and radiation losses of the slotline (SL) can be reduced with a thick BCB encapsulation to enhance the THz signal. The coplanar waveguide (CPW) remains in a medium position. Besides the parasitic mode (SL) and low Q_T problems due to mainly ohmic losses, its major advantage is its planar geometry allowing to an easy circuit integration with THz sources, amplifiers and detectors based on semiconductor. Consequently, these THz studies on BCB microwave standard waveguides open to various perspectives to carry out a broad panel of integrated THz circuits.

Received 26 July 2013, Accepted 16 October 2013, Scheduled 25 October 2013

^{*} Corresponding author: Anne-Sophie Grimault-Jacquin (anne-sophie.grimault@u-psud.fr).

1. INTRODUCTION

In the THz frequency range, waveguides have been traditionally fabricated from metals such as copper, brass, and stainless steel with rectangular, square, and circular cross sections giving total losses at 1 THz as low as 0.7 cm^{-1} (or about 0.3 dB/mm) [1–3]. Attenuation performances of 1.5 m^{-1} (or about 0.0065 dB/mm) between 1 and 2 THz have also been obtained [4] with ferroelectric. Concerning THz dielectric waveguides, attenuation close to 0.004 dB/mm was found [5] in the same frequency range. The lowest losses (0.00001 dB/mm) have been obtained with a highly birefringent polymer (Topas cyclic olefin copolymer (COC) with refractive index 1.53) for terahertz fiber [6].

Although they have interesting properties of dispersion and/or losses, the fabrication and integration of these waveguides with semiconductor based sources, amplifiers and detectors including transistors and diodes, are technologically difficult notably due to their sizes about a few hundreds of microns.

These limitations can be overcome by planar waveguides such as: microstrip [7–9], coplanar waveguide (CPW) [10–12], coplanar stripline (CPS) [10, 13, 14], slotline [15, 16] or the planar Goubau line [17]. But all these waveguides have much more losses than metallic and dielectric waveguides. The origins of these losses are often dielectric, ohmic and radiative.

A low permittivity dielectric substrate as the benzocyclobutene (BCB) can be a rich alternative. It is an interesting thermoset polymer largely considered for high performance electronic integrated circuits (within Si and III/V technologies) and optical applications due to its low dielectric permittivity ϵ_r (2.42), small dielectric loss ($\tan \delta = 7.10^{-3}$ [18]), low optical absorption at telecommunication wavelengths, good charge stability, and excellent thermal resistance. For instance, the Dow Chemical BCB can be easily prepared using spin coating allowing a great control of the layer thickness and subsequent curing for network formation [19] as well as on semiconductor or on metal. When there is back conductor under waveguides, local attachments are sometimes required in the periphery of the circuits support (to avoid any disruption of the line own properties). Moreover, the low BCB permittivity involves low guided dispersive propagation. The THz guided wave can be slowed down close to the substrate transverse electromagnetic wave (TEM) on a broaden frequency range. This was already verified for coplanar transmission lines modeled with ANSOFT HFSS based on finite element method (FEM) from 20 to 1000 GHz. We recently performed a numerical optimization, and the results were compared to S -parameter measurements in the

[340–500] GHz frequency range after a careful de-embedding. A good agreement was found between experimental and numerical results with low attenuation constants 2.7 dB/mm and 3.5 dB/mm at 400 GHz and 500 GHz, respectively. One disadvantage of BCB, compared to the semiconductor material, is that it increases the characteristic impedance (Z_c) of the waveguides at low frequency beyond the standard value $50\ \Omega$ leading to a rise up of the return losses during characterization with a vector network analyzer (VNAs). An extension about a few tens of microns of the waveguide dimensions can alleviate this restraint. Thus, direct comparisons of dispersion and losses between different planar waveguides in THz frequency are not obvious, because they depend on the substrate nature, Z_c [20], or the field confinement width W . Whatever the selective criterion, the dimensions of the waveguides are still free to be optimized.

This article deals with a study of the dispersion, losses and quality factor of four planar waveguides on BCB (microstrip, CPW, stripline and slotline), and some directions to reduce losses are proposed. Section 2 describes the structure of each waveguide and the strategy used in the 3D numerical calculations to analyze dispersions and treat separately the losses. The modeling is performed with two different three-dimensional (3D) electromagnetic (EM) softwares ANSOFT HFSS and CST MWS. These two commercial softwares have been used simultaneously in frequency domain to investigate each waveguide configuration. As demonstrated in [12] with our indigenous code MAXTRA 3D, Ansoft HFSS and CST MW Studio give similar results, but sometimes HFSS overestimates up to ten percents the losses (notably the radiation). That is why the choice to present the results obtained with CST was privileged here. Moreover, the incident waveport dimensions were adjusted by verifying that a maximum of modes is excited. The 3D modeling allows us to verify and isolate the propagation of the fundamental modes. Evanescent modes are thus excluded.

In Sections 3 and 4, quantitative comparisons and optimization of the THz transmission for the four BCB waveguides (CPW, microstrip, stripline and slotline) are presented between 20 and 1000 GHz to find the best suited structure for Z_c fixed to $100\ \Omega$ or not. The advantages, limitations, and performances of each waveguide are studied by modifying the geometry. Conclusions are presented in Section 5.

2. SPECIFICATIONS

2.1. Description of the Four BCB Waveguides

Figure 1 shows the structures and geometric notations of the four planar BCB waveguides investigated.

The microstrip line (Fig. 1(a)) is the most used hyperfrequency (HF) waveguides and has a single conductor ribbon on a dielectric substrate surface and a single ground plane on the other side. At low frequency, its effective permittivity (ϵ_{eff}) depends on the physical dimensions, and it is lower than the dielectric substrate one. Its Z_c can vary from 93 to 210 ohms (for W in $[5-30] \mu\text{m}$) at low frequencies. It is the most robust and much less expensive than traditional waveguide technology, as well as being far lighter and more compact. Various electronic components can be formed from microstrip such as couplers, antennas, filters and power dividers.

CPW (Fig. 1(b)) was first proposed as a monolithic integrated circuit (MIC) transmission line by Wen [21]. It consists of a center strip with two parallel ground planes equidistant from it on either side located on the substrate surface. CPW has low dispersion and support a quasi-TEM dominant mode. At higher frequencies, the field becomes less-TEM, and more transverse electric (TE) in nature. The magnetic field is elliptically polarized (more suitable for nonreciprocal ferrite devices [22] for instance). A second fundamental mode named slotline (SL) also exists. It is qualified as parasitic because it can disturb at high frequency the CPW propagation as the parallel

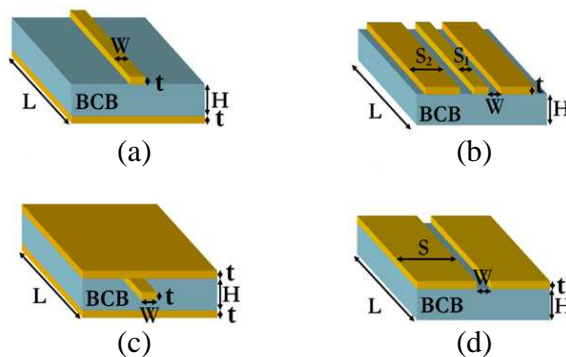


Figure 1. BCB waveguides and notation of dimensions in the simulation: (a) microstrip, (b) coplanar waveguide (CPW), (c) stripline and (d) slotline.

plate mode in a stripline and the higher order transverse electric or magnetic modes in general. When the frequency rises up, the dominant mode can exchange energy by electromagnetic (EM) coupling with another propagating mode. This coupling can be evaluated through a coefficient calculated with overlap integrals of the vector cross product of respective electric and magnetic field of each EM mode as in [12]. Technically, the SL mode for CPW can be attenuated by using air-bridges [23, 24]. Unhappily, bridge ribbons increase insertion losses and make fabrication more difficult. Its Z_c can vary from 73 to 123 ohms (for W in [1.6–12] μm) at low frequencies.

The stripline is the earliest form of planar transmission (Fig. 1(c)). It consists of a strip conductor centered between two parallel ground planes with two equal slabs of a dielectric or ferrite medium separating the center conductor from the ground planes. Usually, the medium is a solid material, but in some applications air is the actual dielectric used. Their good electromagnetic shielding and low attenuation losses are their advantages, which make them suitable for high quality factor Q and low-interference applications. However, striplines require strong symmetry and thereby present difficulties in the design of many circuit functions notably for incorporating chip elements and associated bias circuitry. Any vertical asymmetry in the stripline structure could couple to waveguide-type modes bounded by the ground planes and the side walls. The stripline supports real TEM wave while it is not the case for the other waveguides analyzed in this paper.

However, the maximum operating frequency in this line is limited by the appearance of a higher-order H-type mode. The parallel plate mode can also influence the dominant mode, but it is not the case in a homogeneous dielectric substrate. Z_c of stripline is between 45 and 120 ohms (for 30 μm de BCB and W in [5–30] μm), and it depends on the dielectric constant and on the cross-sectional geometry of the strip center-conductor and ground planes.

The slotline was first proposed by Cohn [25]. Three kinds of slotlines exist unilateral (studied here (Fig. 1(d))), antipodal, and bilateral. The basic unilateral slotline consists of a narrow gap in the conductive coating on one side of the dielectric substrate. The other side of the substrate is bare. It is easy to fabricate because it requires only single-sided board etching. It can be incorporated with microstrip lines for new types of circuits. The substrate concentrates the field (mainly a TE (transverse electric)) density between the plates, but it does not suppress higher order modes or overall radiation, which means that slotline is not usually applicable to broadband applications.

The slotline has a low quality factor Q due to its lossy character and highly dispersive behavior. The ability to provide

elliptic polarization is useful for nonreciprocal ferrite circulators and isolators [22]. Z_c is typically in the range of 95 to 160 ohms for W in [5–30] μm . Z_c increases with slot width. The conductor losses are generally higher than the dielectric losses [3, 16]. They increase with frequency but decrease with slot width.

Implementing such waveguides in the THz range presents the same challenges as in the microwave domain.

2.2. Dimensions of the Four BCB Waveguides

For this study, the length L and thickness t of the conductor ribbons of the lines are respectively 1 mm and 500 nm. The notation W represents the gap width for CPW (Fig. 1(b)) and slotline (Fig. 1(d)), while W stands for the metal width for microstrip (Fig. 1(a)) and stripline (Fig. 1(c)). The BCB height is $H = 30 \mu\text{m}$. In CPW, the central strip width is $S_1 = 10 \mu\text{m}$, and finite ground plane width is $S_2 = 24 \mu\text{m}$. The strip width for slotline is $S = 240 \mu\text{m}$ ($S \gg W$). The parameter W is used as reference geometrical parameter for each waveguide. Indeed, various physical properties namely the characteristic impedance Z_c , phase velocity V_p , and attenuation constant α of the interested dominant mode depend critically on it. Table 1 lists the range of Z_c at 20 GHz through the variation of W within the technological realization limit of the optical lithography. For slotline, the minimum Z_c achieved is around 100Ω with a narrow gap ($W = 5 \mu\text{m}$) due to the small permittivity of BCB. Consequently, $Z_c = 100 \Omega$ appeared as a convenient tradeoff to compare the four waveguides. The specific W of each transmission line corresponding to $Z_c = 100 \Omega$ is also enumerated in (Table 1).

Table 1. Characteristic impedance of BCB waveguides and their dimensions at 100Ω .

Waveguide	Z_c at 20 GHz	W at 100Ω
CPW	73–123 Ω ($W = 1.6 - 12 \mu\text{m}$)	6.6 μm
Microstrip	210–93 Ω ($W = 5 - 30 \mu\text{m}$)	25 μm
Stripline	120–45 Ω ($W = 5 - 30 \mu\text{m}$)	7.3 μm
Slotline	95–160 Ω ($W = 5 - 30 \mu\text{m}$)	6 μm

The optimization of the waveguide performances by changing other parameters besides W , such as the height of the substrate for instance, will also be discussed.

2.3. How Are Dispersions, Losses and Quality Factor Evaluated?

To study separately the origin of each loss, the properties of the substrate and metallic strips are tuned according to values listed in Table 2. For a direct calculation of the attenuation constant α_R due to radiation losses, the conductor is assumed to be quasi electrically perfect (PEC) with a metallic conductivity fixed to the extremely high value of $\sigma_{Au} = 10^{10}$ S/m. The real parts (ϵ_r) of the relative dielectric permittivity of the BCB is 2.42, and the loss tangent is set to zero. A finite conductivity equal to $\sigma_{Au} = 5 \cdot 10^6$ S/m (moderate quality) is assigned to the gold (Au) conductor for the evaluation of conduction loss (α_C). For the dielectric loss (α_D), the loss tangent of BCB $\tan \delta_{BCB}$ is fixed to 0.007 [18] while $\sigma_{Au} = 10^{10}$ S/m. In the total losses ($\alpha_T = \alpha_R + \alpha_D + \alpha_C$), all contributions of conductors and dielectric are included. These various definitions of the materials, notably the metallizations, are chosen in agreement with the reliability of the two softwares as explained in [26].

Table 2. Dielectric and metallic parameters in the calculation of the different losses.

Losses	σ_{Au} (S/m)	$(\tan \delta)_{RCB}$
a_R	10^{10}	0
$a_R + a_C$	$5 \cdot 10^6$	0
$a_R + a_D$	10^{10}	0.007
$a_T = a_R + a_D + a_C$	$5 \cdot 10^6$	0.007

However, the attenuation α_T appears as no longer sufficient for the assessment of the waveguide performances. Another selection criterion namely the quality factor Q_T , as notified in [27], is a relevant and complementary parameter to illustrate them:

$$Q_T = \frac{\beta}{2\alpha_T} \quad (1)$$

$$\frac{1}{Q_T} = \frac{1}{Q_R} + \frac{1}{Q_C} + \frac{1}{Q_D} \quad (2)$$

where β and α_T are the modulus of the propagation vector and total attenuation corresponding to the CPW mode, respectively. Q_T reflects losses as a function of the phase and therefore the wanted electrical length of the line (Eq. (1)). This definition makes sense for high values

of Q_T (> 5), and it is applicable here for frequency exceeding 200 GHz. The inverse of Q_T can also be explained as a sum of the inverses of the quality factors of each kind of losses Q_R (for radiation), Q_C (for ohmic) and Q_D (for dielectric) (Eq. (2)). Indeed, linear attenuation α_T is very useful for investigating the losses per meter (versus the physical length of the line of propagation) introduced by interconnections: the higher the attenuation is, the lower the device performances are in term of the transmitted signal magnitude. In filters, impedance matching networks, power splitters, phase shifters or couplers, quarter-wave or half-wave lines are needed, and it is the electrical length which dictates the operation of these various devices.

3. COMPARISONS OF THE FOUR BCB WAVEGUIDES FOR THE SAME CHARACTERISTIC IMPEDANCE $Z_C = 100 \Omega$

3.1. Dispersions with the Phase Velocity V_p

The dispersion of an EM mode can be investigated via the behavior of its phase velocity V_p versus frequency. Indeed, V_p is directly linked to the propagation vector β as:

$$V_p = \frac{\omega}{\beta} \quad (3)$$

where $\Omega = 2\pi f$, and f is the frequency. In Fig. 2, the phase velocity V_p of the wanted dominant mode of each waveguide on BCB is plotted and assigned by their own W parameter values (see Fig. 1) corresponding to the same characteristic impedance ($Z_c = 100 \Omega$) in the frequency range [20–1000] GHz. In the stripline, V_p is quasi constant and always equals the phase velocity of the free propagating wave in the dielectric BCB ($V_p = 1.93 \cdot 10^8$ m/s), underlying the TEM topology of the wave.

The V_p of the CPW varies from 1% on the whole frequency range, and its dispersion is very slight. On the other hand, the V_p of the microstrip and slotline decrease from 400 GHz and beyond this frequency, and the slope of the curves is steeper for the slotline. Its V_p attenuates from 5.5%, namely one and half times more than microstrip. Thus, this waveguide is the most dispersive. Consequently, the four waveguides can be organized in descending order following their more or less dispersive nature: Slotline > Microstrip > CPW > Stripline. The dispersive character of the slotline and microstrip shows that these waveguides can be used on a narrow frequency band [0–200] GHz (where V_p is regular) unlike the stripline and CPW whose V_p is constant in the frequency range [0–1000] GHz.

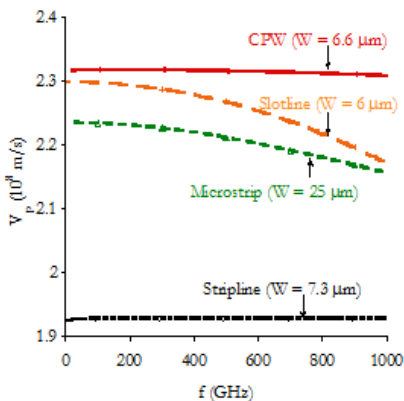


Figure 2. Comparison of the phase velocity V_p of the four waveguides for $Z_c = 100 \Omega$ (Ansoft HFSS and CST Studio MW).

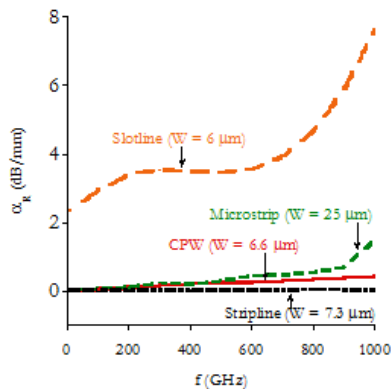


Figure 3. Comparison of the radiation loss α_R of the four waveguides for $Z_c = 100 \Omega$ (Ansoft HFSS and CST Studio MW).

3.2. Discussion of the Attenuations

3.2.1. Radiation Losses α_R

The radiation loss α_R comes from two main contributions. One is due to the coupling between the dominant mode and the other parasitic modes or waves (surface waves in a substrate with finite thickness [28]). The other one comes from the leakage into the substrate side as a shock wave [29–32], when V_p of the dominant mode is higher than the TEM mode in the BCB. Fig. 3 shows the radiation losses α_R of the four waveguides for $Z_c = 100 \Omega$. Only 3D modeling allows addressing radiation losses. Berini was able to quantify the contribution of the leaky modes by a complete 2D approach [30], but these modes are not accessible by the calculation of eigenvalues of the Helmholtz operator over the finite size waveports used by HFSS and CST.

In the stripline α_R is quasi null due to the non-dispersive character of its TEM dominant mode, while the CPW and microstrip have equivalent radiation attenuation below 200 GHz. From 500 GHz, α_R increases in these two transmission lines. In CPW, α_R reaches 0.43 dB/mm at 1 THz following a cubic relation with the frequency as in [10], and in microstrip, α_R equals 1.48 dB/mm at 1 THz. This originates from the shock wave radiation when a V_p mismatch exists between the main propagating mode and the substrate wave. In the

microstrip, when W increases, the EM energy of the main mode is essentially confined in the substrate between the strip and the ground plane making the coupling with the substrate wave stronger. Larger metal width and/or larger frequency promote radiation. The waveguide having the highest radiation losses, ($\alpha_R = 7.63$ dB/mm) at 1 THz, is the most dispersive namely the slotline. SL also features a continuum of radiation modes in air and into the dielectric substrate which can be excited by discontinuities, bends, short-circuits. This property is an advantage for the development of planar antenna, but in term of the transmission, it is a restraint. α_R can be reduced by using narrower slot. But, the fabrication of such a waveguide becomes more difficult, and the characteristic impedance will be altered accordingly. To significantly reduce the attenuation α_R by keeping $Z_c = 100 \Omega$, W spacing must be changed, but this modification should be accomplished by the addition of a supplementary thickness h of polymer above the line, leading to an encapsulation of the slotline. Indeed, as adopted in [16], a supplementary BCB layer of height h (in the inset of the Fig. 4) should be a very interesting way because BCB is more malleable than semiconductors or/and other dielectric materials, and it is technologically easy to spin coated on the top of the line.

To illustrate, radiation losses α_R are plotted versus h and various W in Fig. 4. For slotline with $Z_c = 100 \Omega$, α_R decreases with the increase of h , and it becomes inferior to 1 dB/mm when $h = 60 \mu\text{m}$. For this value, the radiation (total) losses are reduced from 7.63 (9.6) dB/mm to 0.7 (3.49) dB/mm at 1 THz making α_R comparable

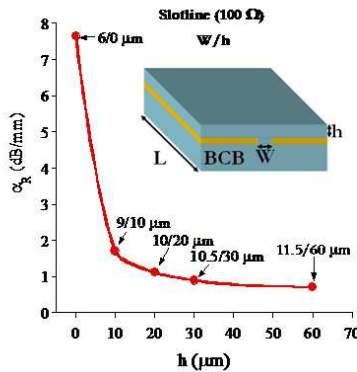


Figure 4. Radiation loss α_R of slotline covered with BCB (thickness h) on the top of the structure for various combinations of W and h at 1 THz for $Z_c = 100 \Omega$ (CST Studio MW).

with dielectric losses for the configuration 11.5/60 μm . A triple-layer of BCB with the ratios (2/3 on the top and 1/3 below) generates a decrease of 90% and 64% of α_R and α_T , respectively. Such a structure has a prominent associated radiation quality factor Q_R attaining 230, which is thirteen times larger than an non-encapsulated structure. $Q_T = 40$ for the combination $(W, h) = (11.5, 60)$ as observed on Fig. 5 where each configuration is presented and compared.

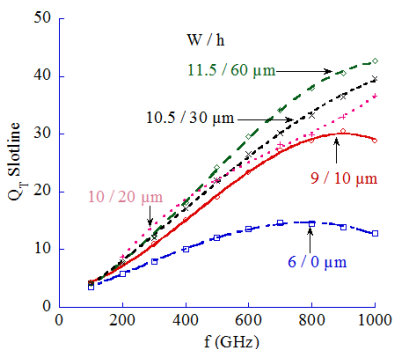


Figure 5. Increase of the total quality factor Q_T of slotline for $Z_c = 100 \Omega$ by deposition of BCB (thickness h) on top of the structure with different combinations of W and h (CST Studio MW).

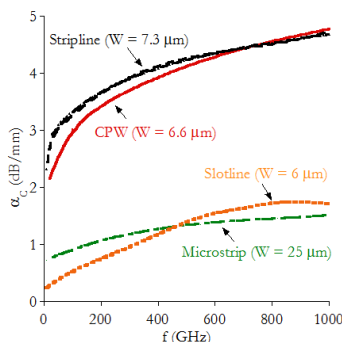


Figure 6. Comparison of the conduction losses α_C of the four waveguides for $Z_c = 100 \Omega$ (Ansoft HFSS and CST Studio MW).

Consequently, the total losses in SL become lower than 0.5 dB/mm in relation to those obtained in microstrip at 1 THz. This is very promising for THz propagation applications.

3.2.2. Conductor Losses α_C

Conductor losses result from the metallic material (strip and ground planes) through the conductivity, skin effect, and surface roughness. Here, losses α_C arise from the finite conductivity (σ) fixed here in the gold metallizations at $\sigma_{Au} = 5 \cdot 10^6 \text{ S/m}$. For each waveguide, they have been calculated and compared in Fig. 6 with Z_c always fixed to 100Ω . α_C follows a function of the square root of the frequency. A row approximation of the conduction losses can be described as proportional to a surface skin resistance R_s which is defined in ohms by

square unit depending on the skin thickness δ as $R_S = 1/(\sigma_{Au}\delta)$ (where $\delta = (\pi f \mu \sigma_{Au})^{-\frac{1}{2}}$, and μ and σ_{Au} are respectively the permeability and the conductivity of metals (strip conductors and ground planes)) [34]. When the frequency increases, R_s also increases. Here, the conductor thickness is under the skin depth for frequency lower than 200 GHz with the chosen conductivity, and this choice of metal thickness is taken for technological reasons. Conductor thickness should be at least three or four times higher than δ . In microstrip, in addition to R_s , α_C depends on the current density normalized by the magnitude of the total intensity integrated in the operating frequency range. The current density is not uniform in the strip and the ground plane. The current density has a tendency to diverge at the strip edges at such a rate that the skin loss is unbounded, which leads to a leakage of the electrical field to the adjacent ground planes. For the slotline, this capacitive effect also occurs, and it is accentuated between the two coupled lines. However, these two waveguides, whose W is respectively defined at 25 and 6 μm , have weaker losses close to 1.7 dB/mm at 1 THz. An alternative to reduce α_C notably is to use high quality conductors or to increase W for each configuration.

The waveguides which suffer from the largest α_C (4.7 dB/mm at 1 THz) are the CPW and the stripline. For these transmission lines, α_C rises when the gap W for CPW or the strip width W for stripline becomes narrow. A solution to reduce α_C in CPW line is that the signal strip and slot width should be of the same order [9, 33]. To maintain $Z_c = 100 \Omega$ for the stripline, both the central metal width (W) and the dielectric thickness (H) should be changed. These dimensions disturb less the values of the radiation and the dielectric losses. Fig. 7 shows the conduction loss α_C versus the variation of the parameter pair W/H in the stripline. Large values of W and H (24/100 or 16/60) are preferred in the frequency range studied. However, in practice, H is constrained by the maximum limit thickness of BCB which can be spin-coated over the metallic ground plane. $H = 60 \mu\text{m}$ appears as a good alternative in step with the fabrication process. The corresponding strip width W is 16 μm . At these values, the conduction (total) losses are reduced by over (or almost) an half from 4.68 (5.64) dB/mm to 2.14 (3.23) dB/mm at 1 THz.

Consequently, α_T of a stripline becomes lower than those (4 dB/mm at 1 THz) of the microstrip ($H = 30 \mu\text{m}$). (The α_T of the other waveguides will be discussed in the Section 3.2.4).

These observations are well confirmed by the calculation of the corresponding conductor quality factor Q_C . Its value is substantial and equals 120 at 1 THz for these two waveguides leading to a total quality factor $Q_T = 63$ and 56 for the couple of parameters 16/60 and

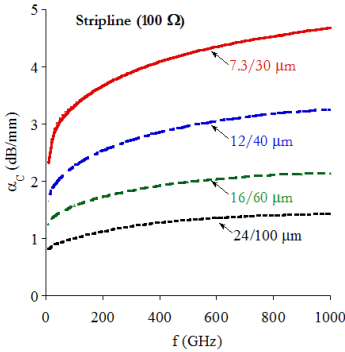


Figure 7. Conduction loss α_C of stripline for $Z_c = 100 \Omega$ with different combinations of dimension parameters W and H (CST Studio MW).

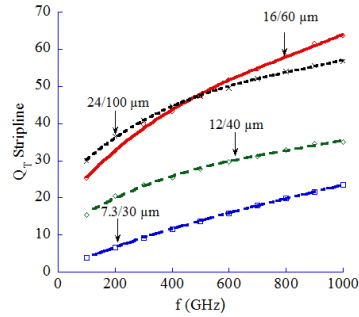


Figure 8. Quality factor Q_T of stripline for $Z_c = 100 \Omega$ with different combinations of W and H (CST Studio MW).

24/100 respectively (Fig. 8). The Q_T of the stripline depends directly on the conductor factor and $\tan \delta$ of BCB following the relation:

$$Q_T = \frac{Q_C}{(1 + Q_C) \tan \delta} \quad (4)$$

This relation is in agreement with the results found with the relation (Eq. (1)).

3.2.3. Dielectric Losses α_D

The dielectric losses α_D are included in BCB via a non-null $\tan \delta$ and can be solely described by a constant phenomenological parameter ($\tan \delta$) extracted from measurement which is sufficient to well treat this kind of losses in the THz frequencies [18]. The corresponding attenuation α_D obtained for each waveguide is thus plotted and compared in Fig. 9.

As predicted at low frequency, α_D changes linearly versus frequency, and the dielectric losses are the highest in stripline up to 1 dB/mm at 1 THz. However, α_D remains always inferior to this value on the entire frequency range, and it is weak for both waveguides in comparison with the radiation and conduction losses. Consequently, α_D plays a minor role in the total attenuation. It can be reduced by employing a substrate material with even lower loss tangent, such as the cyclic-olefin copolymer (COC, $\epsilon_r = 2.35$ at 10 GHz and $\tan \delta = 0.0007$ at 1 THz) [35].

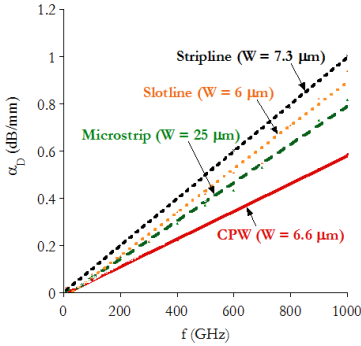


Figure 9. Comparison of the dielectric loss α_D of the four waveguides for $Z_c = 100 \Omega$ (Ansoft HFSS and CST Studio MW).

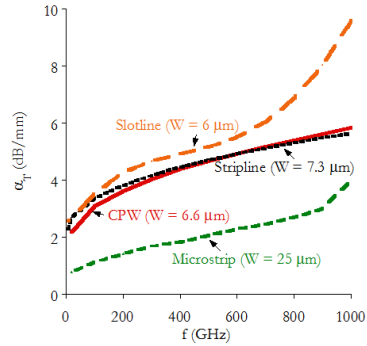


Figure 10. Comparison of the total losses α_T of the four waveguides for $Z_c = 100 \Omega$ (Ansoft HFSS and CST Studio MW).

3.2.4. Total Losses α_T

In Fig. 10, the total losses α_T , which correspond to the sum of the previous three types of losses have been plotted for each planar line. The material properties of BCB and metals are respectively assigned as $\tan \delta_{BCB}$ and $\sigma_{Au} = 5 \cdot 10^6 \text{ S/m}$.

The lowest total attenuation α_T of 3.93 dB/mm at 1 THz is obtained for the microstrip which occurs as the optimal THz waveguide in the frame of this study. This value is inferior to those found for thin film microstrip line (TFMSL) with $\alpha_T = 6 \text{ dB/mm}$ where the BCB thickness is between 1 and 2 μm , and W is in the order of 8 μm [20]. Indeed a decrease of the substrate thickness, while maintaining a constant Z_c , must be accompanied by a narrowing of the conductor width W . But, it must be noticed that a decrease of W leads to higher conductor losses along with a lower Q_T factor. And such dimensions with a small H make the technological realization of this type of waveguide less obvious. Consequently, this solution is not preferred, and a large W equal to or higher than 25 μm is more adequate. The total quality factor Q_T is also plotted for each guide (see Fig. 11). It evolves almost as a parabolic function versus frequency and reaches the best value close to 42 for microstrip.

These values of α_T and Q_T can be optimized through different combinations of the metal width (W) and BCB thickness (H) as shown in Fig. 12. For $W = 35 \mu\text{m}$ and $H = 50 \mu\text{m}$, α_T are lowered

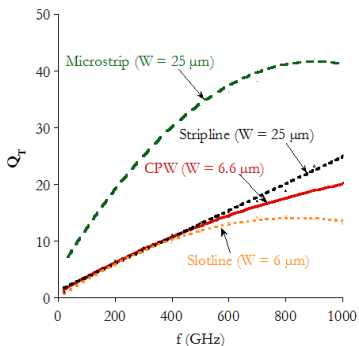


Figure 11. Quality factor Q_T of the four waveguides for $Z_c = 100 \Omega$ (Ansoft HFSS and CST Studio MW).

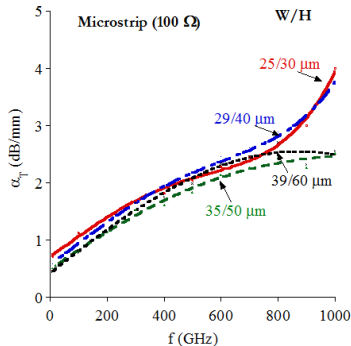


Figure 12. Total losses α_T of microstrip for $Z_c = 100 \Omega$ with different combinations of W and H (Ansoft HFSS).

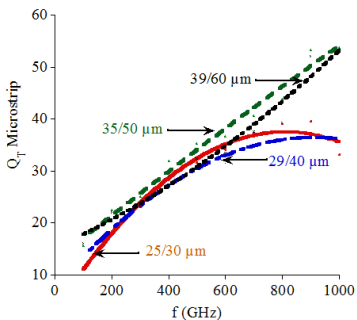


Figure 13. Quality factor Q_T of microstrip for $Z_c = 100 \Omega$ with different combinations of W and H (Ansoft HFSS).

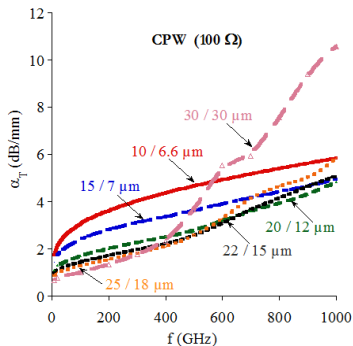


Figure 14. Total losses α_T of CPW for $Z_c = 100 \Omega$ with different combinations of W and H (Ansoft HFSS).

from 4 dB/mm to an optimal value of 2.52 dB/mm at 1 THz, making microstrip still the most preferable THz waveguide.

In microstrip, an enlargement of the metallic ribbon of 30% and a thickening of the BCB layer of 40% leads to an increase of the total quality factor Q_T of 40% (33 to 54) as indicated in Fig. 13.

Whereas, the slotline seems to be the most lossy waveguide with

$\alpha_T = 9.6$ dB/mm at 1 THz (see Fig. 10) and with a maximum Q_T equal to 11 which remains weak (see Fig. 11). As the metallic losses are compensated by the main mode propagation vector up to 800 GHz, the slotline has its Q_T which increases up to 11. Beyond 800 GHz, Q_T is low due to the important rise of the radiation losses (74% of α_T). It is associated to its strong dispersion but also to the dimension W . If the dispersion becomes weak, the radiation loss will decrease accordingly whereas α_D contributes in average between 9 and 20% in α_T . Then, this waveguide is less relevant among all studied transmission lines in this article. The quality factors of two other waveguides CPW and stripline are similar until 400 GHz. Q_T is also controlled by β , and no decay can be observed on the considered frequency range. However, the quality factor of the CPW is lower than that of stripline until 1 THz where $Q_T(\text{CPW}) = 20$ and $Q_T(\text{stripline}) = 25$. It is due to their large metallic conduction losses (≈ 4.7 dB/mm) from which the stripline and the CPW mainly suffer, as indicated in Table 3 where the different losses in each waveguide are summarized at 1 THz and evaluated previously. Indeed, α_C contributes just over 80% in the total attenuation in CPW and stripline.

For the stripline, this can be corrected with different values of W and H evoked before knowing that for this waveguide the radiation losses can be neglected, and α_T boils down to the sum of α_C and α_D .

In the CPW, α_R increases with the gap width W and central metal width S_1 , while α_C decreases with W . Thus, to improve α_C the dimensions S_1 and W should be simultaneously modified in order to keep Z_c fixed to $100\ \Omega$ at 20 GHz. The evolution of the total losses with several combinations (S_1/W) is shown in Fig. 14. The

Table 3. Comparison of losses at 1 THz of the four waveguides for $Z_c = 100\ \Omega$ (Ansoft HFSS and CST Studio MW) without optimization and with $\sigma_{Au} = 5 \cdot 10^6\ \text{S}\cdot\text{m}^{-1}$ and $\tan \delta = 0.007$.

Waveguide	a_R (dB/m)	a_D (dB/m)	a_C (dB/m)
CPW			
($W = 6.6\ \mu\text{m}$)	0.43	0.59	4.77
Microstrip			
($W = 25\ \mu\text{m}$)	1.48	0.82	1.63
Stripline			
($W = 25\ \mu\text{m}$)	0.006	1.00	4.68
Slotline			
($W = 6\ \mu\text{m}$)	7.63	0.94	1.71

optimal dimensions found are: $S_1 = 20 \mu\text{m}$ and $W = 12 \mu\text{m}$. Then, the total losses α_T are reduced from 1 dB/mm namely 5.84 dB/mm to 4.83 dB/mm at 1 THz by switching the CPW with $S_1/W = 10/6.6 \mu\text{m}$ to the optimal structure. If S_1 and W are chosen higher than these optimal values, the radiation losses grow significantly when the frequency is beyond 400 GHz. If they are fixed below the optimal values, it is the conduction losses that dominate in the total attenuation α_T . To complete this analysis, the corresponding quality factor Q_T was also plotted versus frequency in Fig. 15 (the most lossy waveguide ($W = S_1 = 30 \mu\text{m}$) is excluded). The optimal structure described previously is in competition with three other waveguides. Indeed, at high frequency ($> 750 \text{ GHz}$), Q_T of the optimal structure equals 24 and is dominated by the structure with $S_1/W = 15/7$ ($Q_T = 25$) μm and $S_1/W = 10/6.6 \mu\text{m}$ ($Q_T = 24, 8$). The CPW, with $S_1/W = 20/12$, has Q_T which decreases from 800 GHz, due to a slowing down of the propagation vector β of the dominant mode whose Q_T depends also on the propagation vector β (see relation (Eq. (1))). Indeed from 800 GHz, the parasitic mode SL occurs. This frequency is pushed up to 900 GHz in the two other waveguides. At low frequency ($< 200 \text{ GHz}$), it is the CPW with $S_1/W = 25/18 \mu\text{m}$ that has better quality factor $Q_T = 15$ due to its weak conductor losses. Consequently, a compromise should be made following the frequency range to use the most appropriate waveguide. This shows that following the transmission line chosen, the total quality factor can vary from the single to the double at 1 THz. To improve these performances by keeping the same impedance Z_c the geometry of the waveguides should be modified. The parameter W and the height of the substrate are key parameters to decrease the total losses versus frequency. Fig. 16 brings the quality factor Q_T of the best transmission line after their optimization for $Z_c = 100 \Omega$ fixed versus the different combinations of S_1 and W for CPW, W and H for microstrip, stripline and slotline. These various improvements make the stripline as the best waveguide with a $Q_T = 63$ ($W/H = 16/60$) against 54 (35/50) for the microstrip. A tradeoff should be made between the slotline and CPW following the frequency, namely under or above 500 GHz. If other selection criteria are used, the results may differ, but the analysis procedures to optimize the THz propagation are similar. α_R and α_C are the most dominant losses in these waveguides, and they can be controlled by the geometric parameter W because the more the EM field is concentrated along the central ribbon or the slot, the more the performances of the waveguides are improved. Then, the effective width W_{eff} can be chosen as another common parameter without necessarily be combined with the height of the substrate BCB (that remains fixed to $30 \mu\text{m}$). As a consequence, Z_c becomes different

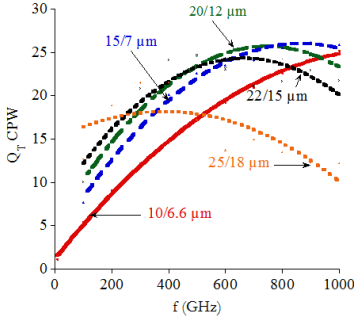


Figure 15. Quality factor Q_T of CPW for $Z_c = 100\ \Omega$ with different combinations of S_1 and W (Ansoft HFSS).

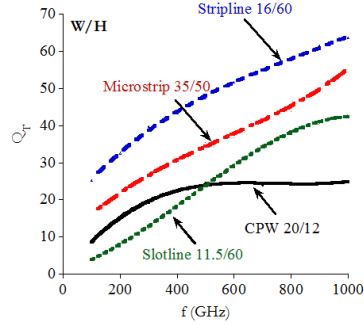


Figure 16. Quality factor Q_T of the best transmission line after their optimization for $Z_c = 100\ \Omega$ fixed with the different combinations of S_1 and W for CPW, W and H for microstrip, stripline and slotline (Ansoft HFSS and CST Studio MW).

for each waveguide. This point is investigated and illustrated via the total losses for the effective width W_{eff} fixed to $30\ \mu\text{m}$ in the following last section.

4. COMPARISON OF THE FOUR BCB WAVEGUIDES AT THE SAME EFFECTIVE WIDTH $W_{eff} = 30\ \mu\text{m}$

In the CPW, W_{eff} corresponds to the sum $S_1 + 2W$ and for the three other waveguides W_{eff} is W . In Fig. 17 the total losses α_T of the four waveguides with $W_{eff} = 30\ \mu\text{m}$ are plotted with the assignment of the respective characteristic impedance. It should be noted that the chosen parameters are not unique. The thickness of the substrate H equals $30\ \mu\text{m}$.

In comparison with Fig. 10 and Fig. 11, again, the microstrip is the best THz waveguide, with $\alpha_T = 2.29\ \text{dB/mm}$ at 1 THz and for $Z_c = 93\ \Omega$. This modification allows a reduction of 10% of α_T in comparison with the best configuration obtained for $W = 35\ \mu\text{m}$ and $H = 50\ \mu\text{m}$ in Fig. 12. In [20], the losses decrease when Z_c increases in microstrip. This behavior is also verified here. In stripline, α_T is 2.88 dB/mm at 1 THz, and this configuration allows a diminution of

11% of α_T versus the configuration $W/H = 10/60 \mu\text{m}$ in Section 3.2.2. Total losses are slightly higher than those in microstrip due to its larger α_C , but its characteristic impedance $Z_c = 45 \Omega$ is interesting because it is close to 50Ω . In CPW ($Z_c = 112 \Omega$), α_T equals 4.71 dB/mm (3% lower than the CPW optimized for $Z_c = 100 \Omega$) at 1 THz, and it is dominated by $\alpha_C = 3.27 \text{ dB/mm}$ at 1 THz. Due to its high dispersion and $\alpha_R = 9.25 \text{ dB/mm}$ at 1 THz, the slotline has the largest attenuation $\alpha_T = 10.46 \text{ dB/mm}$ at 1 THz and remains less efficient.

These observations are confirmed by the analysis of the total quality factor Q_T in Fig. 18. Until 300 GHz, the Q_T of the stripline and the microstrip are similar. Beyond this frequency microstrip is better with $Q_T = 57$ at 1 THz. The losses of the microstrip are decreased by 43% and the Q_T by 6%. The slotline reaches a maximum value of Q_T equal to 10, and this geometric change is less favorable.

The optimization of the attenuation in each waveguide at W_{eff} gives satisfactory results particularly for the stripline. S_1 and W in CPW can be modified at the same time to find the minimum attenuation through a compromise between the radiation and conduction losses. For stripline and microstrip, the BCB thickness (H) can be altered to lower the conduction loss. The spin-coating of a BCB layer on the top of the slotline structure is again an efficient way to reduce the radiation loss.

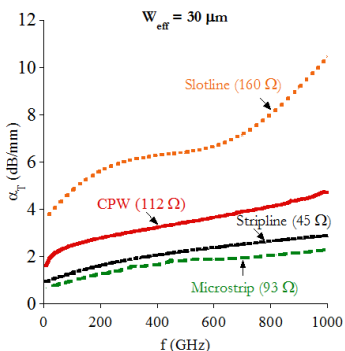


Figure 17. Comparison of the total losses α_T of the four waveguides with $W_{eff} = 30 \mu\text{m}$ ($S_1 = W = 10 \mu\text{m}$ for CPW) (Ansoft HFSS and CST Studio MW).

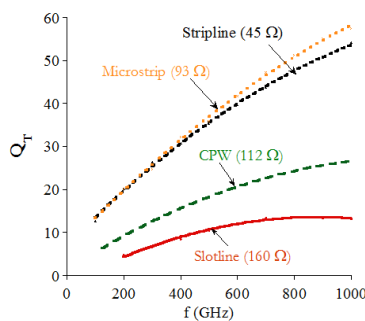


Figure 18. Comparison of the quality factor Q_T of the four waveguides with $W_{eff} = 30 \mu\text{m}$ ($S_1 = W = 10 \mu\text{m}$ for CPW) (Ansoft HFSS and CST Studio MW).

5. CONCLUSION

The dispersion and attenuation of four classical planar microwave waveguides on BCB have been extensively investigated by an original 3D EM numerical approach in the frequency range [20–1000] GHz. 3D modeling allows addressing radiative losses efficiency. The contributions of each loss has been regardless quantified, and solutions to decrease each attenuation have been suggested. Two studies of the losses have been conducted: first for Z_c fixed at $100\ \Omega$ and second for W_{eff} fixed at $30\ \mu\text{m}$. The comparisons among four transmission lines show that each waveguide is mono-mode except the CPW due to the SL mode. Microstrip ($\alpha_T = 2.52\ \text{dB/mm}$ for $Z_c = 100\ \Omega$ and for $W/H = 35/50\ \mu\text{m}$ after optimization and $2.29\ \text{dB/mm}$ for $W = 30\ \mu\text{m}$ at 1 THz with $H = 30\ \mu\text{m}$) and stripline (with quasi-null radiation losses and the best quality factor $Q_T = 63$ for $Z_c = 100\ \Omega$) are the best waveguides for THz signal propagation. The BCB has been proven as a very useful and efficient low losses THz substrate. Slotline suffers from its large dispersion and important α_R (convenient for antenna applications) even with narrow slot. A BCB encapsulation of the waveguide is a very interesting way to solve these drawbacks for the THz signal propagation. Besides the parasitic mode (SL) and low Q_T problems, CPW requires a thick substrate. Its main advantage is its planar geometry which gives the opportunity to be associated with many THz sources and detectors based on semiconductor devices such as diodes or transistors. Consequently, the use of microwave standard microwave metallic waveguides with BCB in THz appears as a performant continuum of the HF technologies. BCB is well suited for THz circuits. As illustrate in [36], transistors embedded in microstrip lines on BCB have been measured by using a multilayer thru-reflect-line (TRL) calibration and coupling corrections to 750 GHz.

ACKNOWLEDGMENT

The authors thank Aloyse Degiron for proofreading and scientific advices provided to improve this paper.

REFERENCES

1. McGowan, R. W., G. Gallot, and D. Grischkowsky, "Propagation of ultrawideband short pulses of terahertz radiation through submillimeter-diameter circular waveguides," *Optics Lett.*, Vol. 24, No. 20, 1431–1433, 1999.

2. Gallot, G., S. P. Jamison, R. W. McGowan, and D. Grischkowsky, "Terahertz waveguides," *J. Opt. Soc. Am. B*, Vol. 17, No. 5, 851–863, 2000.
3. Mendis, R. and D. Grischkowsky, "Undistorted guided-wave propagation of subpicosecond terahertz pulses," *Optics Express*, Vol. 26, No. 11, 846–848, 2001.
4. Hidaka T., H. Minamide, et al., "Ferroelectric PVDF cladding terahertz waveguide," *Proc. SPIE 5135, Optical Information, Data Processing and Storage, and Laser Communication Technologies*, 70–77, 2003.
5. Harrington, J., R. George, P. Pederson, and E. Mueller, "Hollow polycarbonate waveguides with inner Cu coatings for delivery of terahertz radiation," *Optics Express*, Vol. 12, 5263–5268, 2004.
6. Hou, Y., F. Fan, et al., "Highly birefringent polymer terahertz fiber with honeycomb cladding," *Optik*, Vol. 124, 3095–3098, 2013.
7. Byrne, M. B., J. Cunningham, et al. "Terahertz vibrational absorption spectroscopy using microstrip-line waveguides," *Appl. Phys. Lett.*, Vol. 93, 182904, 2008.
8. Byrne, C. M., P. Upadhyaya, M. Lachab, E. H. Linfield, and A. G. Davies, "Terahertz evanescent field microscopy of dielectric materials using on-chip waveguides," *Appl. Phys. Lett.*, Vol. 92, 032903, 2008.
9. Kasai, S., A. Tanabashi, K. Kajiki, et al., "Micro strip line-based on-chip terahertz integrated devices for high sensitivity biosensors," *Appl. Phys. Express*, Vol. 2, 062401, 2009.
10. Frankel, M. Y., S. Gupta, J. A. Valdmanis, and G. A. Mourou, "Terahertz attenuation and dispersion characteristics of coplanar transmission lines," *IEEE Trans. Microw. Theory Techn.*, Vol. 39, No. 6, 910–916, 1991.
11. Lok, L. B., C.-J. Hwang, H. M.-H. Chong, K. Elgaid, and I. G. Thayne, "Measurement and modeling of CPW transmission lines and power dividers on electrically thick GaAs substrate to 220 GHz," *Proc. IRMMW — THz*, 1–2, 2008.
12. Grimault-Jacquín, A.-S., B. Tissafi, E. Perret, and F. Aniel, "Considering to minimize losses in terahertz coplanar waveguide on indium phosphide," *Microw. and Optical Techn. Lett.*, Vol. 54, No. 1, 213–219, 2012.
13. Cheng, H., J. F. Whitaker, T. M. Weller, and L. P. B. Katehi, "Terahertz-bandwidth pulse propagation on a coplanar stripline fabricated on a thin membrane," *IEEE Microw. Guided Wave Lett.*, Vol. 4, No. 3, 89–91, 1994.

14. Kadoya, Y., M. Onuma, S. Yanagi, T. Ohkubo, N. Sato, and J. Kitagawa, "THz wave propagation on strip lines: Devices, properties, and applications," *Radioeng.*, Vol. 17, No. 2, 48–55, 2008.
15. Wachter, M., M. Nagel, and H. Kurz, "Metallic slit waveguide for dispersion-free low-loss terahertz signal transmission," *Appl. Phys. Lett.*, Vol. 90, 061111, 2007.
16. Pahlevaninezhad, H., B. Heshmat, and T. E. Darcie, "Efficient terahertz slot-line waveguides," *Opt. Express*, Vol. 19, No. 26, B41–B55, 2011.
17. Akalin, T., A. Treizebr, and B. Bocquet, "Single-wire transmission lines at terahertz frequencies," *IEEE Trans. Microw. Theory Techn.*, Vol. 54, No. 6, 2762–2767, 2006.
18. Perret, E., N. Zerounian, S. David, and F. Aniel, "Complex permittivity characterization of benzocyclobutene for terahertz applications," *Microelectron. Eng.*, Vol. 85, 2276–2281, 2008.
19. Schwdiauer, E., G. Neugschwandtner, S. Bauer-Gogonea, S. Bauer, and W. Wirges, "Low dielectric constant cross linking polymer: Film electrets with excellent charge stability," *Appl. Phys. Lett.*, Vol. 75, 3998–4000, 1999.
20. Schnieder, F. and W. Heinrich, "Thin-film microstrip lines and coplanar waveguides on semiconductor substrates for sub-mm wave frequencies," *Frequenz*, Vol. 59, 5–6, 1–4, 2005.
21. Wen, C. P., "Coplanar waveguide: A surface strip transmission line suitable for nonreciprocal gyromagnetic device applications," *IEEE Trans. Microwave Theory Tech.*, Vol. 17, 1087–1090, 1969.
22. Maloratsky, L., *RF and Microwave and Integrated Circuits: Passive Components and Control Devices*, Elsevier, 2004, ISBN: 9780080492056.
23. Lee, H., W. Kim, J. Lee, and J. Kim, "Suppression of coupled-slotline mode on CPW Using air-bridges measured by picosecond photoconductive sampling," *IEEE Microw. Guided Wave Lett.*, Vol. 9, No. 7, 265–267, 1999.
24. Jackson, R. W., "Considering in the use of coplanar waveguide for millimeter-wave integrated circuits," *IEEE Trans. Microw. Theory Techn.*, Vol. 34, No. 12, 1450–1456, 1986.
25. Cohn, S. B., "lot-line on a dielectric substrate," *IEEE Trans. on Microwave Theory Tech.*, Vol. 17, 768–778, 1969.
26. Episkopou, E., S. Papantonis, W. Otter, and S. Lucyszyn, "Defining material parameters in commercial EM solvers for arbitrary metal based THz structures," *IEEE Trans. on THz*

- Science and Tech.*, Vol. 2, 513524, 2012.
27. Hsu, H. P., "On the general relation between α and Q ," *IEEE Transactions on Microw. Theory and Techniques*, Vol. 11, No. 4, 258–258, 1963.
 28. Collinm, R. E., *Field Theory of Guided Waves*, McGraw-Hill, New York, 1960.
 29. Rutledge, D. B., D. P. Neikirk, and D. P. Kasilingam, "Integrated circuit antennas," *Infrared and Millimeter Waves*, Vol. 10, Academic Press, New York, 1983.
 30. Berini, P., "Plasmon-polariton waves guided by thin lossy metal films of finite width: Bound modes of symmetric structures," *Phys. Rev. B*, Vol. 61, 10484–10503, 2000.
 31. Grischkowsky, D., I. N. Duling III, J. C. Chen, and C. C. Chi, "Electromagnetic shock waves from transmission lines," *Phys. Rev. Lett.*, Vol. 59, No. 15, 1663–1666, 1987.
 32. Jelley, J. V., *Cerenkov Radiation and Its Applications*, Pergamon Press, New York, 1958, ISBN: 0-08-013127-1.
 33. Ke, J.-Y. and C. H. Chen, "The coplanar waveguides with finite metal thickness and conductivity," *IEEE MTT Digest*, TH4B-1, 1681–1684, 1994.
 34. Gupta, K. C., R. Garg, R. Bahl, and P. Bhartia, *Microstrip Lines and Slotlines*, 2nd Edition, Artech House, 1996, ISBN: 0-89006-766-X.
 35. Peytavit, E., C. Donche, S. Lepilliet, G. Ducournau, and J.-F. Lampin, "Thin-film transmission lines using cyclic olefin copolymer for millimeter-wave and terahertz integrated circuits," *Electron. Lett.*, Vol. 47, No. 7, 2011.
 36. Williams, D. F., "A prescription for sub-millimeter-wave transistor characterization," *IEEE Trans. on THz Science and Technol.*, Vol. 3, No. 4, 433–439, 2013.